Steam gasification behavior of tropical agrowaste: A new modeling approach based on the inorganic composition

Lina Maria Romero Millan, Fabio Emiro Sierra Vargas, Ange Nzihou

Steam gasification behavior of tropical agrowaste: A new modeling approach based on the inorganic composition

Lina María Romero Millán[a,b,*], Fabio Emiro Sierra Vargas[a], Ange Nzihou[b]

[a] Universidad Nacional de Colombia – Sede Bogotá, Facultad de Ingeniería, Ciudad Universitaria, Bogotá, Colombia
[b] Université de Toulouse, Mines Albi, CNRS, Centre RAPSODEE, Campus Jarlard, Route de Teillet, F.81013 Albi Cedex 09, France

Keywords:
Catalytic impact
Inorganic composition
Kinetic modeling
Steam gasification
Tropical lignocellulosic biomass

A B S T R A C T

The steam gasification and co-gasification reactivity and kinetics of coconut shells, oil palm shells and bamboo guadua were studied from an isothermal thermogravimetric analysis, with temperatures ranging from 750 °C to 900 °C, and steam partial pressures from 3 to 10 kPa. In the analyzed experimental range, inorganics were identified as the most influential parameter in biomass reactivity and kinetics. Accordingly, a new modeling approach is proposed to predict the gasification behavior of lignocellulosic agrowaste based on their inorganic composition. A good agreement between the experimental and modeled data was found, showing that the proposed approach is suitable for the description and prediction of the gasification behavior of biomasses with different macromolecular structure and within a wide range of inorganic composition, and H/C and O/C ratios near 1.5 and 0.8 respectively. This kinetic model could constitute a valuable tool for reactor design and scale-up of steam gasification facilities using tropical lignocellulosic feedstocks.

1. Introduction

Tropical regions are rich in biodiversity thanks to their geographic location and climate conditions. In this regard, they are appropriate for the development of agricultural activities and cultivation of a great variety of crops. Several developing countries in tropical regions base their economy in agriculture and farming and produce great amounts of agro-wastes that usually remain under-exploited. These residues could be valorized as biofuels or transformed into value-added products, giving new development opportunities for local communities.

In this regard, gasification is a very interesting thermochemical process for the recovery of energy from agrowaste. In particular, steam gasification produces high heating value fuel gases that can be used for the generation of heat and power [1–4]. However, the valorization of agrowaste could have some restrictions. One of the most important is probably the fact that agricultural residues availability often depends on seasonal crops. Consequently, most gasification facilities should operate intermittently, or work with different kind of residues or even blends.

Several authors have highlighted the differences in the gasification behavior of chars from different biomasses. In particular, the inorganic elements are reported to be the most influential parameter in the steam gasification reactivity and conversion profile [5,6]. Alkali and alkali earth metals (AAEM) like K, Na, Ca and Mg, which are present in indigenous biomass could have a catalytic effect on biomass gasification [7]. Among these elements, K has been reported to be the most active species for steam and CO_2 gasification of charcoal and biomass [8,9]. In contrast, Si, Al or P may inhibit this catalytic effect, as they tend to react with AAEM [10,11].

Most studies related to the impact of inorganics in the gasification behavior of biomasses use impregnation techniques to modify the composition of the samples [8,12–15]. In general, these treatments allow a good understanding of the effects of inorganics on gasification. However, the behavior of impregnated inorganic elements may differ from the one of inorganic elements in their natural form and distribution in biomass. In this regard, Dupont et al. [16] studied 21 samples of woody biomasses, confirming the beneficial impact of K and the inhibitory effect of Si in the indigenous biomass.

Generally, authors analyze the gasification behavior of biomasses individually. Nevertheless, most gasification applications in developing countries should work with different kind of residues or blends depending on their availability. In this context, the understanding of the impact of biomass characteristics and blends interactions in their gasification behavior is important in order to properly adapt the process parameters and conditions to the application.

To describe the steam gasification behavior of biomasses, several

* Corresponding author at: Universidad Nacional de Colombia – Sede Bogotá, Facultad de Ingeniería, Ciudad Universitaria, Bogotá, Colombia. Université de Toulouse, Mines Albi, CNRS, Centre RAPSODEE, Campus Jarlard, Route de Teillet, F.81013 Albi Cedex 09, France.
E-mail addresses: lina.romero_millan@mines-albi.fr, lmromerom@unal.edu.co (L.M. Romero Millán).

Nomenclature

α	degree of conversion or reaction extent (−)
A	frequency factor or pre-exponential factor (min^{-1})
BG	bamboo guadua
CS	coconut shells
$d\alpha/dt$	decomposition rate (−)
daf	dry ash free
E_a	activation energy (kJ/mol)
OPS	oil palm shells
PH_2O	steam partial pressure (kPa)
R	ideal gas constant: 8.3144 J/mol K
t	time (min)
T	temperature (°C, K)

authors have proposed different kinetic approaches, some of them incorporating the impact of inorganic elements. In this regard, Kajita et al. [17] considered that gasification occurs in a parallel reaction scheme and developed a dual Langmuir-Hinshelwood model, identifying K as the main catalytic element. This study highlighted the beneficial impact of K, but did not deal with other inorganic elements present in biomasses. For their part, Zhang et al. [10] analyzed the influence of AAEM and Si in the gasification behavior of different biomasses. They proposed a modified random pore model, introducing two dimensionless parameters that depends on the inorganic content of samples. Even when the calculation method of these parameters was not explicitly presented, the authors concluded that the gasification reactivities of biomasses are governed mainly by the amount of inorganic species. More recently, Dupont et al. [6] proposed a kinetic approach with two different kinetic laws for biomasses with inorganic ratio K/Si + P > 1 and K/Si + P < 1. A zeroth-order and a volumetric first-order model were found to describe the behavior of samples, respectively. Furthermore, in the case of biomasses with K/Si + P > 1, the authors suggest that the gasification kinetics can be predicted simply through the knowledge of the K content of the sample. Even when the proposed approach in this work can satisfactorily estimate the behavior of biomasses within a wide range of inorganic compositions, the conversion of samples with intermediate values of inorganic ratio (K/Si + P ≈ 1) is not completely described. The authors stated that the decomposition of these biomasses can be estimated either with a zeroth or a first order law. Additionally, concerning the analysis of the simultaneous steam gasification of different kind of biomasses and their kinetic modeling, no studies have been found in the literature until now.

Accordingly, the aim of this work is to study the steam gasification behavior of three tropical lignocellulosic biomasses and their blends, from an isothermal thermogravimetric analysis. The influence of the gasification temperature and steam partial pressure on the gasification reactivity of biomasses was discussed. Also, the impact of biomasses and blends composition on the gasification reactivity and kinetics was analyzed. An approach using model-free isoconversional methods and generalized master plots was used to determine the gasification kinetic parameters of the samples and compare their decomposition behavior. As a result, a new model with a unique kinetic equation is proposed to describe and predict the steam gasification behavior of tropical lignocellulosic agrowastes based on their inorganic composition.

2. Materials and methods

2.1. Biomass samples

Three tropical lignocellulosic feedstocks were selected for this study: oil palm shells (OPS), coconut shells (CS) and bamboo guadua (BG). The samples were collected in Colombia, South America, and were provided by a palm oil extraction plant, a food processing industry, and a furniture and handicraft construction site, respectively. The origin of selected samples has been detailed on a previous work [18]. The chemical composition of the biomasses was determined according to the standards of solid biofuels with at least three replicates, and is presented in Tables 1 and 2.

Elemental composition (C, H, N, S, and O) was determined using a Themoquest NA 2000 elemental analyzer, while inorganic speciation was determined using an HORIBA Jobin Yvon Ultima 2 inductively coupled plasma optical emission spectrometer (ICP-OES), based on EN 16967 standard. Proximate analysis was calculated according to the standards EN ISO 18134-3, EN ISO 18123 and EN ISO 18122, respectively. Molecular composition of the biomasses is referred to literature reported values [19–21].

The raw biomasses were milled and sieved to a size range between 100 μm and 150 μm before TGA. The characteristic time analysis of the experiments showed that under the presented conditions, limitations by heat or mass transfer can be neglected. Bi-component biomass blends were prepared after milling and sieving using different proportions.

2.2. Isothermal TGA gasification experiments

Raw biomasses and biomass blends gasification under steam was performed using a Seratam TG-ATD 92 thermal analyzer, coupled with a Wetsys humid gas generator. Approximately 20 mg of each sample were placed in an aluminum crucible and heated from 25 °C to the final gasification temperature (750 °C, 800 °C and 900 °C) at a heating rate of 10 °C/min, under an inert atmosphere. After 10 min, the measured mass loss of the sample was below 0.01%/min and then, it was considered that the pyrolysis stage has finished. The atmosphere was then switched to a mixture of H_2O/N_2 (steam partial pressure from 3.7 kPa to 10 kPa). The total flow rate was 4 L/h for all the experiments.

TGA experiments were conducted twice and averaged to verify their repeatability. A blank test was made for each experimental condition to exclude buoyancy effects. For each experimental condition, the repeatability was found to be satisfactory, as the calculated standard deviation of the mass loss was below 1%.

2.3. Reactivity and kinetic study

2.3.1. Theoretical background

The isothermal gasification experiments described are the basis of the kinetic analysis of biomasses decomposition under a steam atmosphere. The degree of conversion or reaction extent during gasification is defined as in Eq. (1):

Table 1
Organic composition of studied biomasses.

		OPS	CS	BG
Elemental Analysis (wt% daf)	C	46.7 ± 0.2	46.8 ± 0.2	42.7 ± 0.3
	H	6.5 ± 0.1	5.8 ± 0.1	5.4 ± 0.1
	O*	46.2 ± 0.1	47.1 ± 0.1	51.5 ± 0.1
	N	0.6 ± 0.1	0.3 ± 0.1	0.4 ± 0.1
	O/C	0.7 ± 0.1	0.7 ± 0.1	0.9 ± 0.1
	H/C	1.7 ± 0.1	1.5 ± 0.1	1.5 ± 0.1
Proximate analysis (wt% dry basis)	Volatile Matter	77.2 ± 0.3	79.5 ± 0.3	75.1 ± 0.2
	Fixed Carbon*	20.9 ± 0.3	19.1 ± 0.2	19.9 ± 0.3
	Ash	1.7 ± 0.2	1.4 ± 0.1	5.0 ± 0.4
Molecular composition (wt % daf)	Cellulose	30.4	32.5	53.9
	Hemicellulose	12.7	20.5	13.5
	Lignin	49.8	36.5	25.1

* Calculated by difference.

Table 2
Inorganic composition of studied biomasses.

		OPS	CS	BG
Inorganic composition (mg/kg dry biomass)	Al	1 500 ± 22	262 ± 8	243 ± 34
	Ca	54 ± 6	391 ± 73	441 ± 99
	Fe	107 ± 4	160 ± 28	116 ± 17
	K	1 006 ± 15	2 808 ± 44	5 360 ± 85
	Mg	135 ± 3	170 ± 15	173 ± 10
	Na	1.5 ± 0.5	33 ± 11	2 ± 0.8
	P	270 ± 7	397 ± 40	829 ± 62
	Si	5 600 ± 39	309 ± 43	19 372 ± 354

$$\alpha(t) = \frac{m_0 - m(t)}{m_0 - m_f} \tag{1}$$

where m_0 is the mass of the sample at the beginning of the gasification stage, m_f the final mass, and m the current mass at a given time. According to this, the apparent gasification reactivity can be defined as a function of the conversion degree α:

$$R(\alpha) = \frac{1}{1-\alpha} \cdot \frac{d\alpha}{dt} \tag{2}$$

Moreover, the gasification reaction rate $d\alpha/dt$ can described as in Eq. (3):

$$\frac{d\alpha}{dt} = k(T)h(P_{H_2O})f(\alpha) \tag{3}$$

where $k(T)$ is the Arrhenius equation, representing the temperature dependence of the process, $h(P)$ the relation expressing the gasification agent partial pressure dependence, and $f(\alpha)$ the reaction model function representing how the solid state decomposition process occurs. Different authors have suggested that the influence of the reactive atmosphere partial pressure in the reaction rate is described by a power law with a constant exponent value, for almost all conversion levels [22–24].

According to this, the reaction rate can be then written as follows:

$$\frac{d\alpha}{dt} = A\exp(-E_a/RT)P_{H_2O}^n f(\alpha) \tag{4}$$

2.3.2. Isoconversional model free approach

In this study, an isoconversional model-free approach was used to determine the Arrhenius parameters of steam gasification of biomasses. Isoconversional methods are based on the hypothesis that the reaction rate at a constant degree of conversion is only a function of temperature and pressure, and then, the activation energy of the process can be calculated without a previous assumption of the reaction model [24,25]. Also, the dependency of E_a with α can give information about the existence of a single-step or multi-step kinetics [26].

Besides the calculation of the apparent activation energy, the appropriate determination of the decomposition model describing the process is also important, as the wrong assumption of the decomposition mechanism could cause the misestimation of the kinetic parameters and an inaccurate interpretation of the process.

For biomass and coal gasification, three models are generally used in the literature for the description of char conversion. The volumetric model (VM), the shrinking core model (SCM), and the random pore model (RPM). Several studies have shown good agreement between experimental results and the three presented models, regardless of the differences in their theoretical background [27–30]. However, as there is not any relationship established between the biomass characteristics and the decomposition mechanism, no theoretical models were presupposed in this study. Isoconversional model-free methods and the generalized master-plots approach were used for the selection of the reaction expression that better describes the steam gasification process [31,32]. Some solid-state reaction models used for char gasification or combustion description are presented in Table 3.

For isothermal experiments, the reduced-generalized reaction rate expression $\lambda(\alpha)$ in Eq. (5) can be simplified and calculated without the previous knowledge of the activation energy E_a.

$$\lambda(\alpha) = \frac{f(\alpha)}{f(\alpha)_{\alpha=0.5}} = \frac{d\alpha/dt}{(d\alpha/dt)_{0.5}} \frac{exp(E_a/RT)}{exp(E_a/RT_{0.5})} \tag{5}$$

The most suitable $f(\alpha)$ model can be then identified as the best match between the experimental $\lambda(\alpha)$ values and the master-plots calculated from theoretical models. The generalized master-plots of the reaction models presented in Table 3 and calculated according to Eq. (5), are presented in Fig. 1.

3. Results and discussion

3.1. Impact of temperature and steam partial pressure on gasification reactivity

Fig. 2 presents the conversion degree α as a function of time of coconut shells (CS), at three different gasification temperatures and a steam partial pressure of 3.7 kPa. It is possible to observe that the gasification conversion rate is highly dependent on the temperature. An increase in the gasification temperature is associated with a reduction of the time required to reach a specific conversion degree. Accordingly, shorter reaction times are related to higher gasification reactivities.

In this regard, Table 4 summarizes the steam gasification reactivity and reaction time at a conversion degree of 50% for the three raw biomasses analyzed. For all the samples, it is possible to observe that higher gasification temperatures are associated to higher reactivities and shorter reaction times. For instance, it is possible to notice that a temperature rise from 750 °C to 800 °C, increases twice the steam gasification reactivity of CS. Moreover, at 900 °C, its reactivity is 6.6 times higher compared to 800 °C. The same trend was observed for BG and OPS.

The results obtained in the analyzed temperature range are in accordance with those presented in the literature. As already described by several authors for CO_2 and steam atmospheres, at higher temperatures,

Table 3
Most common reaction mechanisms used in solid state kinetic analysis [24,26].

Model		$f(\alpha)$	$g(\alpha)$
Order based	Or1 – First order	$1-\alpha$	$-\ln(1-\alpha)$
	Or2 – Second order	$(1-\alpha)^2$	$[1/(1-\alpha)]-1$
	Or3 – Third order	$(1-\alpha)^3$	$1/2[1/(1-\alpha)^2]-1$
	Or n – nth order	$(1-\alpha)^n$	$[1/(n-1)][(1-\alpha)^{(1-n)}-1]$
Diffusion	D1 – One dimensional	$1/(2\alpha)$	α^2
	D2 – two dimensional	$[-\ln(1-\alpha)]^{-1}$	$\alpha+(1-\alpha)\ln(1-\alpha)$
	D3 – Three dimensional	$(3/2)(1-\alpha)^{2/3}[1-(1-\alpha)^{1/3}]^{-1}$	$[1-(1-\alpha)^{1/3}]^2$
Geometrical contraction	R2 – Contracting area	$2(1-\alpha)^{1/2}$	$1-(1-\alpha)^{1/2}$
	R3 – Contracting volume	$3(1-\alpha)^{2/3}$	$1-(1-\alpha)^{1/3}$

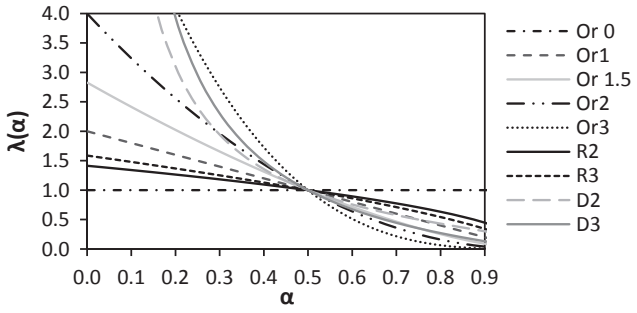

Fig. 1. Generalized master-plots of the reaction models presented in Table 1, calculated according to Eq. (5).

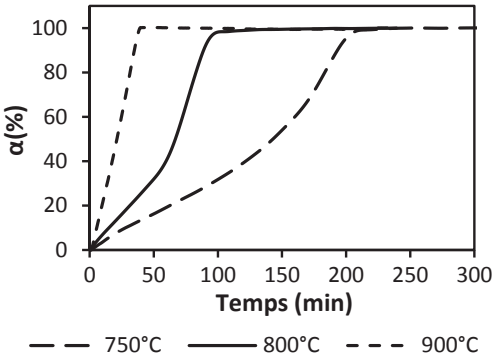

Fig. 2. Conversion degree α vs. time of coconut shells (CS) at three different gasification temperatures and a steam partial pressure of 3.7 kPa.

the gasification process requires shorter times to be completed [33–36].

Regarding steam partial pressure, the conversion profile of coconut shells (CS) can be observed in Fig. 3 at three different steam partial pressures and an intermediate gasification temperature of 800 °C. It can be noticed that an augmentation of this parameter is also associated with a decrease in the reaction time. Indeed, a higher steam partial pressure indicates a greater steam quantity available to react during the gasification stage, explaining the increase in the gasification rate of biomasses. At 800 °C, CS reactivity at a conversion degree of 50% increased from 3.2 min^{-1} to 4.2 min^{-1} with a steam partial pressure rise from 3.7 kPa to 10 kPa. For its part, reaction time decreased from 67 min to 32 min, respectively. As observed with temperature, at higher steam partial pressures, the gasification process requires shorter times to be completed.

According to this and considering Eq. (4), it is possible to determine the exponent *n* of the power law describing the influence of the steam partial pressure PH_2O on the reaction rate. For each conversion degree, this value was calculated from the slope of the plot ln *(dα/dt)* vs ln *(PH_2O)*, using at least three gasification conditions. For the three raw biomasses analyzed, *n* remained nearly constant during all the conversion range, with a mean value of 0.5 and a standard deviation of 0.1. This result is in agreement with the values reported by different authors between 0.4 and 0.8 for steam gasification of biomass and coal [16,22,37].

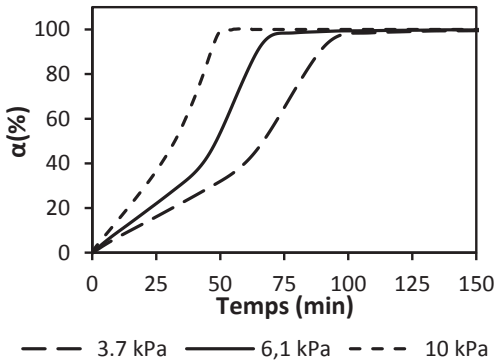

Fig. 3. Conversion degree α vs. time of coconut shells (CS) at three different steam partial pressures and 800 °C.

3.2. Impact of feedstock characteristics on steam gasification reactivity

The impact of the feedstock characteristics on the steam gasification reactivity was studied comparing the behavior of the three selected materials and their blends under different gasification conditions. As an example, the conversion profile of the raw biomasses at a gasification temperature of 800 °C and a steam partial pressure of 3.7 kPa is presented in Fig. 4. It is possible to notice that the behavior of the three samples is notably different. In particular, CS conversion rate is nearly constant and tends to increase at high conversion levels, while OPS and BG conversion rate seems to decrease with time. This behavior was the same under all the analyzed experimental conditions.

Therefore, the gasification behavior does not seem to be related to the macromolecular composition of biomasses. Even when the hemicellulose, cellulose and lignin content of coconut shells and oil palm shells are similar, their gasification conversion profiles are clearly different. Moreover, the behavior of oil palm shells and bamboo guadua are quite similar.

To better understand this, the Fig. 5 shows the conversion profile of coconut shells (CS) and bamboo guadua (BG), at three different gasification temperatures and a steam partial pressures of 10 kPa.

For the analyzed experimental conditions, it can be noticed that CS conversion rate is nearly constant and tends to increase at high conversion levels, as described previously. In contrast, BG conversion rate seems to decrease with time. Also, it can be observed that for a specific conversion degree, there is an important difference in the reaction time of both biomasses. For instance, at 800 °C and 10 kPa, CS total conversion was reached after 55 min, while BG took more than 300 min. This behavior shows that CS have a higher gasification reactivity compared to BG. The reactivity of the three selected biomasses was already highlighted in Table 4. It was possible to observe that CS reactivity is always higher compared with BG and OPS.

These differences can be related to the inherent inorganic content of raw biomasses. In particular, it is possible to notice from Table 2, that coconut shells contain mainly K, Ca, Al and P, while oil palm shells and bamboo guadua are composed mainly of Si, Al, Ca and a little K. Different authors have identified the impact of inorganic elements in biomass gasification. Particularly, the catalytic effect of alkaline and alkaline earth metals (AAEM), and the inhibitory impact of Si, Al and P

Table 4
Steam gasification reactivity and reaction time at 50% conversion. Steam partial pressure 3.7 kPa.

Sample	750 °C		800 °C		900 °C	
	Reactivity (% min^{-1})	Reaction time (min)	Reactivity (% min^{-1})	Reaction time (min)	Reactivity (% min^{-1})	Reaction time (min)
100%CS	0.5	142.8	1.3	66.7	8.7	21.0
100%BG	0.2	234.6	0.7	83.4	4.1	21.5
100%OPS	0.2	236.4	0.5	127.8	2.5	24.8

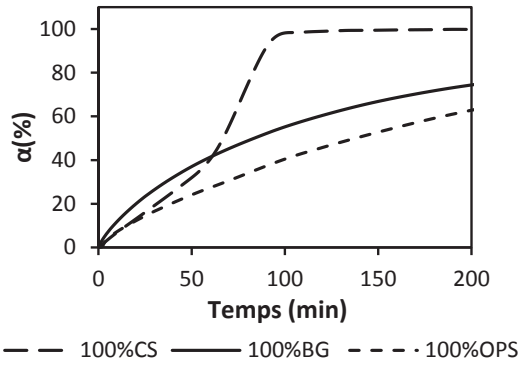

Fig. 4. Conversion profile of the selected biomasses at 800 °C and a steam partial pressure of 3.7 kPa.

[10,17,38]. In this regard, Dupont et al. [6], proposed a relevant correlation between the biomass gasification behavior and the inorganic ratio K/(Si + P). They found that biomasses with K/(Si + P) above 1 show a constant decomposition rate with a slightly increase at high conversion, while biomasses with K/(Si + P) below 1 have a decreasing rate along the whole conversion. According to this and taking into account that K has been reported to have the most beneficial impact on gasification reactivity among AAEM [39], the inorganic ratio K/(Si + P) will be used in this study to characterize and compare the inorganic composition of the selected biomasses.

The observed gasification behavior of the three analyzed biomasses may suggest that despite the differences in the macromolecular constituents, the inorganic composition of samples is the most important parameter that influences their steam gasification behavior. To better understand this impact, the gasification of different biomass blends was also studied. The inorganic ratio K/(Si + P) was calculated for each sample and is presented in Table 5.

From experiments, it was possible to notice that the behavior of biomass blends is not clearly related to the mass blending ratio, but to the inorganic composition of the blend, calculated from the inorganic content of the individual samples.

The analysis of the gasification conversion profiles, showed that the behavior of blends is not additive, if compared to raw biomasses. Moreover, it is not possible to describe synergistic or inhibitory effects as a function of the biomass blend ratio. Since limitations by heat or mass transfer can be neglected under the presented experimental conditions, this behavior suggests that the interactions between biomasses are notably related to their inorganic content. For the analyzed biomasses and blends, it was noted that the conversion rate increased with the K/(Si + P) ratio of the sample. In this regard, a linear relationship was found between the biomass reactivity and the inorganic ratio K/(Si + P) of samples, in the analyzed temperature range, as observed in Fig. 6. This result, confirms the fact that the inorganic species of the biomasses have an impact on their gasification behavior. The

Table 5
Calculated inorganic ratio K/Si + P of analyzed biomasses and blends.

Biomass/blend	K/(Si + P) (−)
100% CS	3.98
100% BG	0.20
100% OPS	0.17
90%CS – 10%BG	1.18
85%CS – 15%BG	0.92
75%CS – 25%BG	0.61
50%CS – 50%BG	0.39
90%CS – 10%OPS	2.15
85%CS – 15%OPS	1.71
75%CS – 25%OPS	1.03
50%CS – 50%OPS	0.58

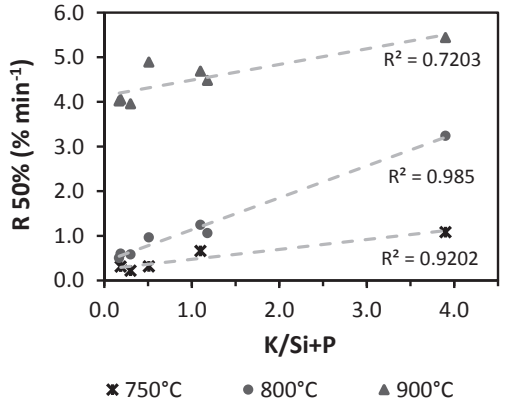

Fig. 6. Steam gasification reactivity at a conversion degree of 50% of biomasses and blends at different temperatures and a steam partial pressure of 3.7 kPa.

gasification reactivity increases with the inorganic ratio, highlighting the beneficial effect of K. In contrast, higher quantities of Si and P could react with K and other AAEM, inhibiting their impact in gasification reactions, and reducing the biomass gasification reactivity.

This observation may have an important impact in real gasification applications. As already discussed, biomasses with lower reactivities require longer gasification times or higher working temperatures to achieve a desired conversion level, impacting the energy consumption of the process. Thus, according to the feedstock characteristics, the process parameters and conditions should be properly adapted.

3.3. Steam gasification kinetic analysis

To better understand the impact of the inorganic composition on the biomass gasification behavior, a kinetic analysis was performed. As already presented, the decomposition curves (α Vs t) of biomasses or blends were analyzed using isoconversional methods in order to

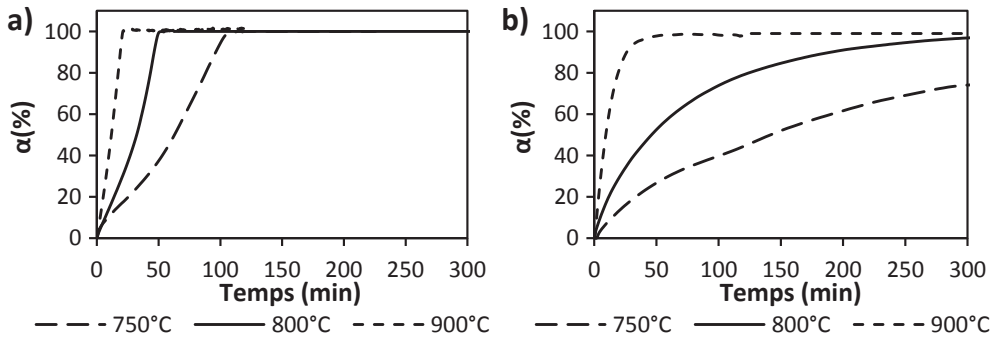

Fig. 5. Conversion degree vs. time of CS and BG at different gasification temperatures. a) CS – 10 kPa, b) BG – 10 kPa.

determine their kinetic triplet E_a, A and $f(\alpha)$.

Firstly, the most suitable reaction model that describes the biomasses gasification was determined using the generalized master plots approach. In general, it was observed that for all the analyzed materials, the decomposition model that best fit the gasification behavior is independent of the temperature and the steam partial pressure. This is the case for many solid-state reactions and was expected for steam gasification [26]. To better understand and compare the differences in the identified reaction models, the gasification behavior of the samples was described as a reaction order model, where n is the reaction order with respect to the reacting solid, as presented in Table 3.

As already stated, for the analyzed biomasses and blends, it was observed that the identified reaction model depends on the inorganic composition. Fig. 7a shows that the feedstocks with inorganic ratio closer or higher than 1 match closely the theoretical plot of a zeroth-order model (Or0) in almost all the conversion range. This result is in accordance with different authors that found that catalytic gasification can be properly described by a reaction order 0 with respect to the reactive solid [17,40,41]. The divergences observed at conversion levels above 60% are possibly related to the catalytic impact of K that becomes more evident at the end of the gasification, when the relative proportion of inorganics compared to carbon is higher.

In contrast, it can be noticed that for the biomasses and blends with inorganic ratio below 1 the most suitable reaction model identified with generalized master plots varies. With the decrease of the inorganic ratio, the reaction model moves away from a zeroth-order model and goes towards a second-order model. From Fig. 7b–d it is possible to observe that BG behavior is close to a reaction order 1.5, while the blends 50%CS–50%BG and 75%CS–25%BG approach a reaction order 1 and 0.7 respectively.

From these results, it can be noticed that there is a linear and inverse relationship between the identified order of reaction and the inorganic ratio of the sample, as presented in Fig. 8.

The observed increase in the reaction order with the decrease in the inorganic ratio could be related to the inhibition of K catalytic impact by Si and P. The higher the Si and P content, the stronger the inhibition impact, and then, the lower the gasification reaction rate. This trend is in accordance with related studies which found that Si and P tend to react with AAEM reducing their catalytic impact in gasification behavior [39].

Similarly, in the case of samples with K/(Si + P) higher that one,

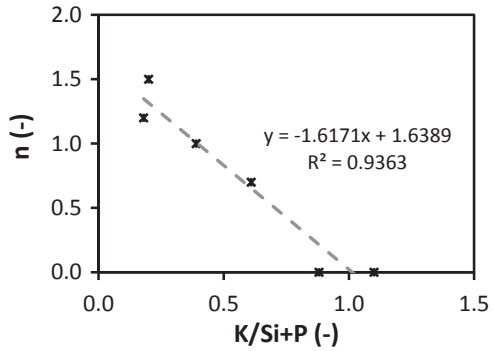

Fig. 8. Identified reaction order vs. inorganic ratio of analyzed samples.

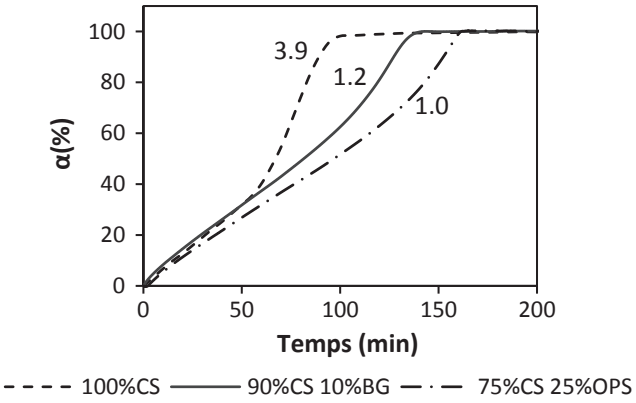

Fig. 9. Conversion profile of different samples with inorganic ratio higher than 1 at 800 °C and 3.7 kPa. The calculated inorganic ratio of the samples is indicated next to each curve.

the catalytic impact of steam gasification also depends on the inorganic ratio. Fig. 9 shows that even when all the samples seem to follow a zeroth order reaction, the higher the K/(Si + P) content, the stronger the catalytic effect. Consequently, the total gasification time was the lowest for the biomass with the highest inorganic ratio. Moreover, the acceleration of gasification rate at the end of the conversion is more important for the biomass with the highest inorganic ratio. As already

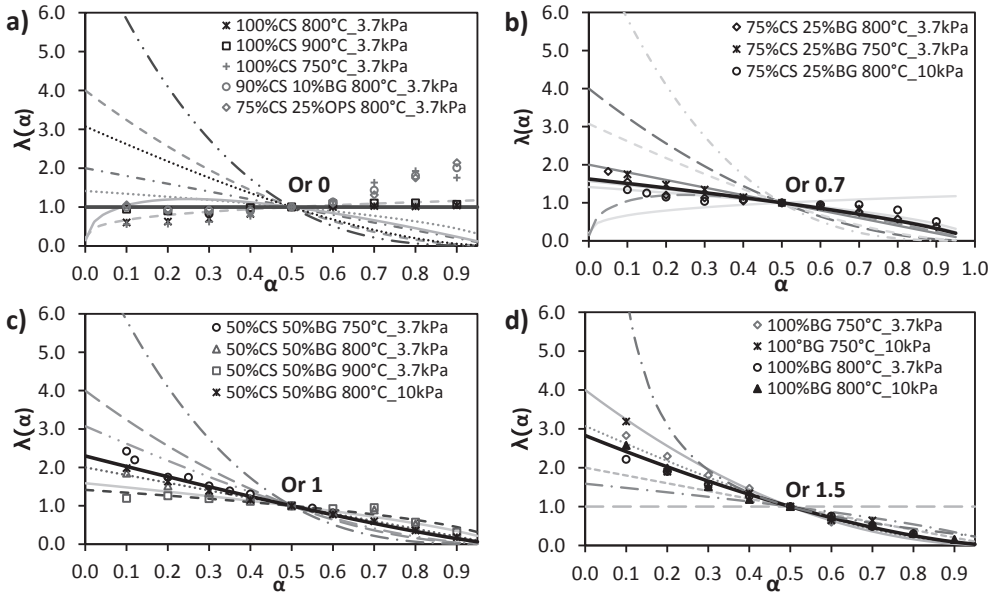

Fig. 7. Comparison between the theoretical and experimental master plots of some analyzed samples and blends.

discussed, this behavior is possibly related to the catalytic impact of K that becomes more evident when the relative proportion of inorganics compared to carbon is higher.

According to these results and in agreement to previous work in the literature, it is possible to say that the steam gasification behavior of biomasses with K/(Si + P) below one follow a non-catalytic mechanism, contrary to biomasses with K/(Si + P) higher than one. The variation in the reaction order identified could be due to the interactions between the inorganic constituents of the biomass. In particular, Si and P could react with K and other AAEM to form alkali silicates, restraining their catalytic impact [10].

After the identification of the appropriate reaction model, the apparent activation energy E_a was determined from the slope of the isoconversional plots regression lines. For all the analyzed samples, the mean apparent E_a calculated was 134 kJ/mol, with a variation coefficient of 6% between the samples. The apparent activation energy calculated in this study is in agreement with different values reported in the literature for biomass steam gasification [16,36,42,43].

According to Fig. 10, no relationship was found between the apparent activation energy and the inorganic coefficient of biomasses and blends. For all the analyzed samples, the calculated E_a remained almost constant with the reaction extent α, with variation coefficients below 15%. This result indicates that the E_a and the reaction model selected using master-plots approach are suitable for the description of the samples gasification during all the conversion range. Finally, the pre-exponential factor was determined from Eq. (4). A mean value of $1.35 \times 10^4\,\mathrm{min}^{-1}\,\mathrm{kPa}^{-0.5}$ was calculated for all the analyzed biomasses and blends. From these results, a kinetic equation that describes the behavior of biomasses and blends as a function of their inorganic content is proposed:

$$\frac{d\alpha}{dt} = 13500 exp\left(\frac{-134000}{RT}\right) P^{0.5}(1-\alpha)^{n} k_1 \tag{6a}$$

where P is the steam partial pressure, n the theoretical model reaction order, and k_1 a coefficient that takes into account the differences observed between the gasification reaction rate of the biomasses that follow a zeroth-order model. Thus, the reaction order n and the coefficient k_1 depends on the inorganic ratio K/(Si + P) as follows: If K/(Si + P) ≥ 1

$$n = 0 \tag{7b}$$

$$k_1 = 0.15\left(\frac{K}{Si + P}\right) + 0.7 \tag{7c}$$

If K/(Si + P) < 1

$$n = -1.62\left(\frac{K}{Si + P}\right) + 1.64 \tag{7d}$$

$$k_1 = 1 \tag{7e}$$

Unlike the existing models that propose different kinetic laws for catalytic and non-catalytic gasification [6,17], it is worth mentioning that the presented kinetic equation (Eq. (6a)) allows the description of the steam gasification behavior of biomasses within a wide range of inorganic compositions, including those with an inorganic ratio close to 1. Moreover, the coefficient k_1 was found to be proportional to the inorganic ratio K/(Si + P) and not to the K content, for the samples that follow a zeroth-order model. In this regard, the presented kinetic approach facilitates the understanding of the influence of biomass inorganic species and their interactions, on the steam gasification process. Furthermore, it confirms the validity of the inorganic ratio K/Si + P proposed by Hognon et al. [38] to describe biomasses and predict their steam gasification behavior.

The proposed kinetic equation was validated and used to reproduce the gasification behavior of the studied biomasses and their blends. For all the analyzed samples and gasification conditions, a good agreement was found between the experimental and the calculated data.

The fit error E was determined according to Eq. (8),

$$E(\%) = 100\left(\frac{\sqrt{\left(\left(\frac{d\alpha}{dt}\right)_{exp} - \left(\frac{d\alpha}{dt}\right)_{calc}\right)^2}}{(\sqrt{N})\left(\frac{d\alpha}{dt}\right)_{exp,max}}\right) \tag{8}$$

where $d\alpha/dt$ are the experimental and calculated values of the decomposition rate, and N is the total number of experimental points [44].

The calculated fitting error was below 7% in all cases. This value was considered reasonable, taking into account the heterogeneity of the biomasses and the incertitude in the measurement of their inorganic composition. Fig. 11 shows the comparison between the experimental results and the model predictions of some analyzed samples. From this figure, it can be noticed that the conversion behavior of biomasses and blends is well described by the proposed kinetic model, highlighting the impact of inorganic composition on the steam gasification kinetics of lignocellulosic biomasses. The low fitting error showed that the presented kinetic equation (Eq. (6a)) is suitable for the description and prediction of the gasification behavior of biomasses or blends based on their inorganic composition.

4. Conclusion

The steam gasification of coconut shells (CS), oil palms shells (OPS) and bamboo guadua (BG) was analyzed under different experimental conditions. Despite the differences in their macromolecular composition, inorganics showed to be the most important parameter influencing the biomass gasification reactivity and kinetics. The results confirmed the beneficial impact of K in gasification and the inhibitory effect of Si and P. Accordingly, a new kinetic equation considering the inorganic composition of feedstocks was proposed. This approach proved to be suitable for the description and prediction of the gasification behavior of lignocellulosic biomasses within a wide range of inorganic compositions, and H/C and O/C ratios near 1.5 and 0.8 respectively. Furthermore, it was evidenced that the co-gasification behavior of biomasses in the presented range can be predicted from the inorganic composition of the individual feedstocks. In future work, the presented approach can be expanded to other lignocellulosic residues and a wider range of blends.

As a result, the proposed kinetic model could constitute a valuable tool for reactor design and for the development and scale-up of steam gasification facilities using tropical lignocellulosic feedstocks. In particular, taking into account that residual biomass availability is variable, this approach could be useful in applications where different kind of residues should be gasified at the same time.

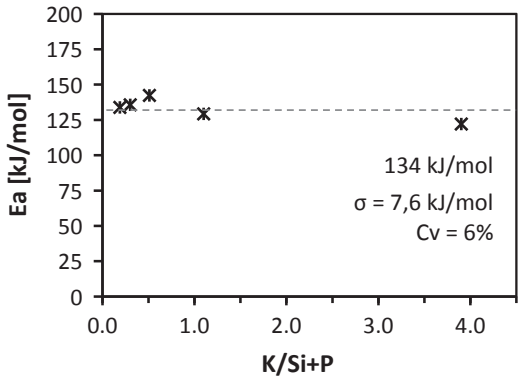

Fig. 10. Apparent activation energy of analyzed samples as a function of the inorganic ratio.

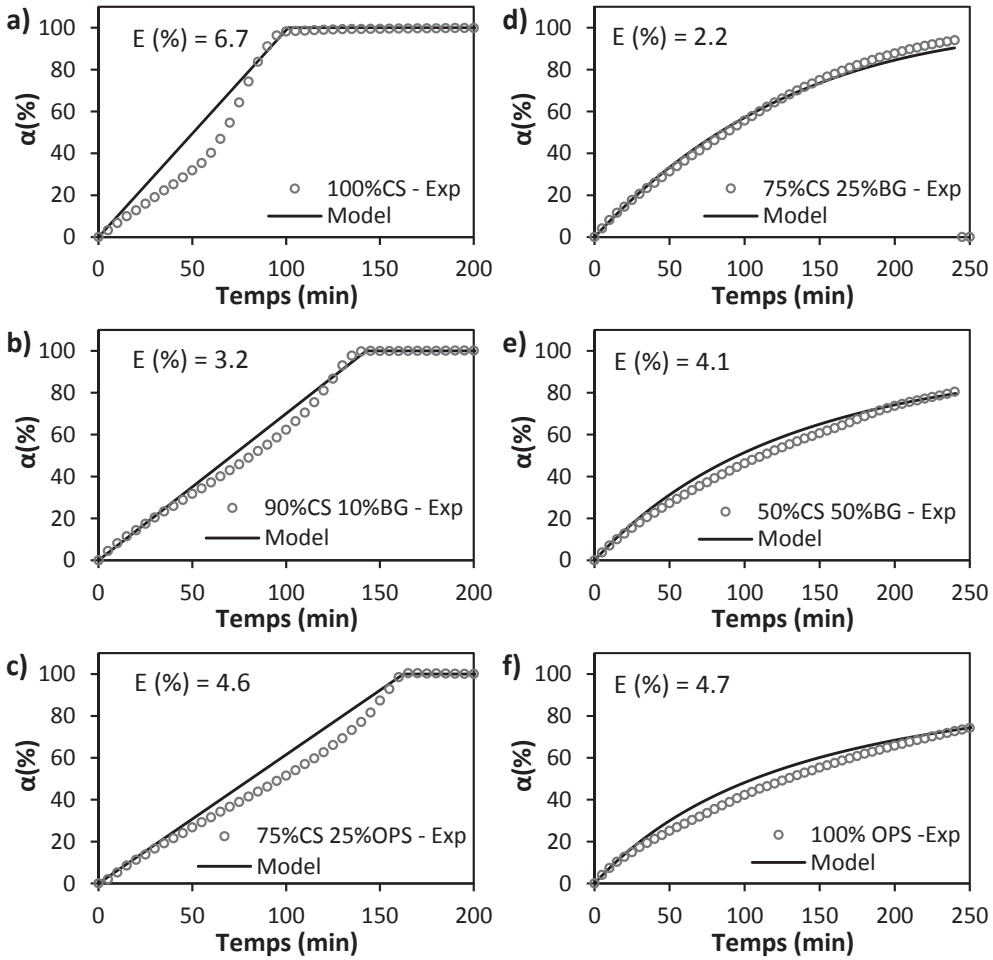

Fig. 11. Comparison between the experimental and modeled decomposition curves of analyzed samples at 800 °C and 3.7 kPa.

Acknowledgements

The authors gratefully acknowledge COLCIENCIAS, for the doctoral scholarship awarded in the frame of the Colombian National Program for Doctoral Formation 647-2014.

Funding

This work was supported by COLCIENCIAS through the Colombian National Program for Doctoral Formation. [Grant 647-2014].

Conflict of interest

There are no conflicts to declare.

References

[1] Basu P. Gasification theory. Biomass gasification, pyrolysis and torrefaction. Elsevier Inc.; 2013. p. 199–248. doi:10.1016/B978-0-12-396488-5.00007-1.

[2] Martínez JD, Mahkamov K, Andrade RV, Silva Lora EE. Syngas production in downdraft biomass gasifiers and its application using internal combustion engines. Renew Energy 2012;38:1–9. https://doi.org/10.1016/j.renene.2011.07.035.

[3] Pereira EG, Da Silva JN, De Oliveira JL, MacHado CS. Sustainable energy: a review of gasification technologies. Renewable Sustainable Energy Rev 2012;16:4753–62. https://doi.org/10.1016/j.rser.2012.04.023.

[4] Sattar A, Leeke GA, Hornung A, Wood J. Steam gasification of rapeseed, wood, sewage sludge and miscanthus biochars for the production of a hydrogen-rich syngas. Biomass Bioenergy 2014;69:276–86. https://doi.org/10.1016/j.biombioe.2014.07.025.

[5] Di Blasi C. Combustion and gasification rates of lignocellulosic chars. Prog Energy Combust Sci 2009;35:121–40. https://doi.org/10.1016/j.pecs.2008.08.001.

[6] Dupont C, Jacob S, Marrakchy KO, Hognon C, Grateau M, Labalette F, et al. How inorganic elements of biomass influence char steam gasification kinetics. Energy 2016;109:430–5. https://doi.org/10.1016/j.energy.2016.04.094.

[7] Encinar JM, Gonzalez JF, Rodriguez JJ, Ramiro MJ. Catalysed and uncatalysed steam gasification of eucalyptus char: influence of variables and kinetic study. Fuel 2001;80:2025–36.

[8] Perander M, Demartini N, Brink A, Kramb J, Karlström O, Hemming J, et al. Catalytic effect of Ca and K on CO 2 gasification of spruce wood char. FUEL 2015;150:464–72. https://doi.org/10.1016/j.fuel.2015.02.062.

[9] Huang Y, Yin X, Wu C, Wang C, Xie J, Zhou Z, et al. Effects of metal catalysts on CO 2 gasification reactivity of biomass char. Biotechnol Adv 2009;27:568–72. https://doi.org/10.1016/j.biotechadv.2009.04.013.

[10] Zhang Y, Ashizawa M, Kajitani S, Miura K. Proposal of a semi-empirical kinetic model to reconcile with gasification reactivity profiles of biomass chars. Fuel 2008;87:475–81. https://doi.org/10.1016/j.fuel.2007.04.026.

[11] Umeki K, Moilanen A, Gómez-Barea A, Konttinen J. A model of biomass char gasification describing the change in catalytic activity of ash; 2012. doi:10.1016/j.cej.2012.07.025.

[12] Kirtania K, Axelsson J, Matsakas L, Christakopoulos P, Umeki K, Furusj E. Kinetic study of catalytic gasification of wood char impregnated with different alkali salts. Energy 2017;118:1055–65. https://doi.org/10.1016/j.energy.2016.10.134.

[13] Jia S, Ning S, Ying H, Sun Y, Xu W, Yin H. High quality syngas production from catalytic gasification of woodchip char. Energy Convers Manage 2017;151:457–64. https://doi.org/10.1016/j.enconman.2017.09.008.

[14] Kramb J, Konttinen J, Gómez-Barea A, Moilanen A, Umeki K. Modeling biomass char gasification kinetics for improving prediction of carbon conversion in a fluidized bed gasifier; 2014. doi:10.1016/j.fuel.2014.04.014.

[15] Kramb J, Demartini N, Perander M, Moilanen A, Konttinen J. Modeling of the catalytic effects of potassium and calcium on spruce wood gasification in CO 2; 2016. doi:10.1016/j.fuproc.2016.01.031.

[16] Dupont C, Nocquet T, Da Costa JA, Verne-Tournon C. Kinetic modelling of steam gasification of various woody biomass chars: Influence of inorganic elements. Bioresour Technol 2011;102:9743–8. https://doi.org/10.1016/j.biortech.2011.07.016.

[17] Kajita M, Kimura T, Norinaga K, Li C-Z, Hayashi J-I. Catalytic and Noncatalytic Mechanisms in Steam Gasification of Char from the Pyrolysis of Biomass; 2009. doi:10.1021/ef900513a.

[18] Romero Millan LM, Sierra Vargas FE, Nzihou A. Kinetic analysis of tropical

lignocellulosic agrowaste pyrolysis. BioEnergy Res 2017. https://doi.org/10.1007/s12155-017-9844-5.
[19] Cuéllar A, Muñoz I. Fibra de guadua como refuerzo de matrices poliméricas – bamboo fiber reinforcement for polymer matrix. Dyna 2010;77:137–42. https://doi.org/10.15446/dyna.
[20] Mortley Q, Mellowes WA, Thomas S. Activated carbons from materials of varying morphological structure. Themochim Acta 1988;129:173–86. https://doi.org/10.1016/0040-6031(88)87334-9.
[21] García-Núñez JA, García-Pérez M, Das KC. Determination of kinetic parameters of thermal degradation of palm oil mill by-products using thermogravimetric analysis and differential scanning calorimetry. Trans ASABE 2008;51:547–57. https://doi.org/10.13031/2013.24354.
[22] Marquez-Montesinos F, Cordero T, Rodriguez-Mirasol Rodriguez J. CO2 and steam gasification of a grapefruit skin char. Fuel 2002;81:423–9.
[23] Morin M, Pécate S, Masi E, Hémati M. Kinetic study and modelling of char combustion in TGA in isothermal conditions. Fuel 2017;203:522–36. https://doi.org/10.1016/j.fuel.2017.04.134.
[24] Vyazovkin S, Burnham AK, Criado JM, Pérez-Maqueda LA, Popescu C, Sbirrazzuoli N. ICTAC kinetics committee recommendations for performing kinetic computations on thermal analysis data. Thermochim Acta 2011;520:1–19. https://doi.org/10.1016/j.tca.2011.03.034.
[25] Šimon P. Isoconversional methods fundamentals, meaning and application. J Therm Anal Calorim 2004;76:123–32.
[26] Brown ME. Handbook of Thermal Analysis and Calorimetry. Volume 1. Principles and Practice. First ed. Elsevier; 1998.
[27] Ahmed II, Gupta AK. Kinetics of woodchips char gasification with steam and carbon dioxide. Appl Energy 2011;88:1613–9. https://doi.org/10.1016/j.apenergy.2010.11.007.
[28] Lopez G, Alvarez J, Amutio M, Arregi A, Bilbao J, Olazar M. Assessment of steam gasification kinetics of the char from lignocellulosic biomass in a conical spouted bed reactor. Energy 2016;107:493–501. https://doi.org/10.1016/j.energy.2016.04.040.
[29] Samdani G, Ganesh A, Aghalayam P, Sapru RK, Lohar BL, Mahajani S. Kinetics of heterogeneous reactions with coal in context of underground coal gasification; 2017. doi:10.1016/j.fuel.2017.02.088.
[30] Tanner J, Bhattacharya S. Kinetics of CO 2 and steam gasification of Victorian brown coal chars. Chem Eng J 2016;285:331–40. https://doi.org/10.1016/j.cej.2015.09.106.
[31] Gotor FJ, Criado JM, Malek J, Koga N. Kinetic analysis of solid-state reactions: the universality of master plots for analyzing isothermal and nonisothermal experiments. J Phys Chem A 2000:10777–82. https://doi.org/10.1021/jp0022205.
[32] Sánchez-Jiménez PE, Pérez-Maqueda LA, Perejón A, Criado JM. Generalized master plots as a straightforward approach for determining the kinetic model: the case of cellulose pyrolysis. Thermochim Acta 2013;552:54–9. https://doi.org/10.1016/j.tca.2012.11.003.
[33] Ye DP, Agnew JB, Zhang DK. Gasification of a South Australian low-rank coal with carbon dioxide and steam: kinetics and reactivity studies. Fuel 1998;77:1209–19. https://doi.org/10.1016/S0016-2361(98)00014-3.
[34] Everson RC, Neomagus HWJP, Kaitano R, Falcon R, Du Cann VM. Properties of high ash coal-char particles derived from inertinite-rich coal: II. Gasification kinetics with carbon dioxide; 2008. doi:10.1016/j.fuel.2008.05.019.
[35] Yip K, Tian F, Hayashi J-I, Wu H. Effect of alkali and alkaline earth metallic species on biochar reactivity and syngas compositions during steam gasification; 2009. doi:10.1021/ef900534n.
[36] Le C, Kolaczkowski S. Steam gasification of a refuse derived char: reactivity and kinetics. Chem Eng Res Des 2015;102:389–98. https://doi.org/10.1016/j.cherd.2015.07.004.
[37] Massoudi Farid M, Jeong HJ, Hwang J. Co-gasification of coal-biomass blended char with CO2 and H2O: effect of partial pressure of the gasifying agent on reaction kinetics. Fuel 2015;162:234–8. https://doi.org/10.1016/j.fuel.2015.09.011.
[38] Hognon C, Dupont C, Grateau M, Delrue F. Comparison of steam gasification reactivity of algal and lignocellulosic biomass: influence of inorganic elements. Bioresour Technol 2014;164:347–53. https://doi.org/10.1016/j.biortech.2014.04.111.
[39] Nzihou A, Stanmore B, Sharrock P. A review of catalysts for the gasification of biomass char, with some reference to coal. Energy 2013;58:305–17. https://doi.org/10.1016/j.energy.2013.05.057.
[40] Bayarsaikhan B, Hayashi J-I, Shimada T, Sathe C, Li C-Z, Tsutsumi A, et al. Kinetics of steam gasification of nascent char from rapid pyrolysis of a Victorian brown coal; 2005. doi:10.1016/j.fuel.2005.02.008.
[41] Shahbaz M, Yusup S, Inayat A, Patrick DO, Ammar M. The influence of catalysts in biomass steam gasification and catalytic potential of coal bottom ash in biomass steam gasification: a review; 2017. doi:10.1016/j.rser.2017.01.153.
[42] Valor WB, Adamon DGF, Fagbémi LA, Bensakhria A, Sanya EA. Comparison of Kinetic Models for Carbon Dioxide and Steam Gasification of Rice Husk Char. Waste Biomass Valorization n.d.;0. doi:10.1007/s12649-017-0054-3.
[43] Guizani C, Sanz FJE, Salvador S. The gasification reactivity of high-heating-rate chars in single and mixed atmospheres of H2O and CO2. Fuel 2013;108:812–23. https://doi.org/10.1016/j.fuel.2013.02.027.
[44] Anca-Couce A, Zobel N, Berger A, Behrendt F. Smouldering of pine wood: kinetics and reaction heats. Combust Flame 2012;159:1708–19. https://doi.org/10.1016/j.combustflame.2011.11.015.